Available online at www.sciencedirect.com
ScienceDirect
Mendeleev Commun., 2023, **33**, 682–685

Mendeleev Communications

Microwave-assisted synthesis of thiazolothiazole-containing conjugated polymers as promising charge-transport materials for perovskite solar cells

Alina V. Lolaeva,[a] Aleksandra N. Zhivchikova,[a,b] Marina M. Tepliakova,[b] Mikhail V. Gapanovich,[a,c] Evgenia O. Perepelitsina,[a] Azaliia F. Akhkiamova,[a,d] Dimitri A. Ivanov,[a,d,e,f] Nikita A. Slesarenko,[a] Albert G. Nasibulin,[b] Alexander V. Akkuratov[a] and Ilya E. Kuznetsov*[a]

[a] *Federal Research Center of Problems of Chemical Physics and Medicinal Chemistry, Russian Academy of Sciences, 142432 Chernogolovka, Moscow Region, Russian Federation. E-mail: kusnetsovilja@gmail.com*
[b] *Skolkovo Institute of Science and Technology, 143026 Moscow, Russian Federation*
[c] *Department of Fundamental Physical and Chemical Engineering, M. V. Lomonosov Moscow State University, 119991 Moscow, Russian Federation*
[d] *Department of Chemistry, M. V. Lomonosov Moscow State University, 119991 Moscow, Russian Federation*
[e] *Institut de Sciences des Matériaux de Mulhouse (CNRS UMR 7361), Université de Haute Alsace, 68057 Mulhouse, France*
[f] *Sirius University of Science and Technology, 354340 Sochi, Russian Federation*

DOI: 10.1016/j.mencom.2023.09.029

The synthesis of novel thiazolo[5,4-*d*]thiazole-containing conjugated polymer was performed by three alternative methods, namely, by the Stille or Suzuki cross-coupling as well as microwave-assisted condensation reaction with carbonyl precursor and dithioxamide. The latter way is straightforward and efficient for the design of novel materials with desirable optoelectronic and physicochemical characteristics providing an encouraging hole-transport properties and comparable performance of perovskite solar cells.

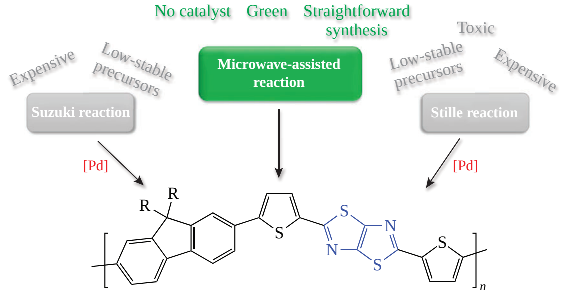

Keywords: thiazolo[5,4-*d*]thiazole, cross-coupling, dithioxamide, green chemistry, microwave-assisted polymerization, perovskite solar cells, hole-transport materials.

Conjugated polymers are promising semiconductor materials for organic solar cells,[1,2] hybrid perovskite solar cells,[3,4] organic field-effect transistors,[5] or electrochromic devices.[6] However, the synthesis of conjugated polymers by the conventional Stille or Suzuki cross-coupling reactions is complex and multistage process involving utilization of expensive and low-stable precursors and catalysts, as well as toxic organotin derivatives,[7] so they are not good for industrial-scale production. Therefore, exploration of alternative and scalable approaches for the preparation of semiconductor polymers is topical.

Thiazolo[5,4-*d*]thiazole (TzTz), an electron-deficient fused (bi)heterocyclic system with high oxidative stability and a rigid planar structure enabling efficient intermolecular π–π overlapping, is a promising building block for the design of organic semiconductors.[8] Enhanced intermolecular interactions of TzTz-containing compounds in solid state provide improved charge carrier mobility. Conjugated polymers with TzTz moiety can be prepared by the Stille or Suzuki polycondensation reactions[9,10] or by condensation of carbonyl,[11] carboxyl,[12] cyano derivatives[13] with dithioxamide (rubeanic acid).[14] The motivation of our work was to comparably investigate palladium-catalyzed cross-coupling reactions and alternative microwave-assisted synthetic approach for obtaining conjugated polymers based on thiophene, fluorene, and thiazolo[5,4-*d*]thiazole (Scheme 1). The polymers obtained by the Stille, Suzuki cross-coupling reactions and by the microwave-assisted condensation are denoted as **P–St**, **P–Sz**, and **P–C**, respectively. We consider that the condensation of carbonyl derivatives and dithioxamide with the formation of thiazolothiazole cycle should be promising. This condensation can be performed either thermally or under microwave irradiation,[15] with the second method usually providing higher yields due to milder reaction conditions.[16] The investigation of hole mobilities of three materials (**P–St**, **P–Sz**, **P–C**) and using them as hole-transport materials in perovskite solar cells revealed that the polymer **P–C** provides comparable properties and power conversion efficiency of devices, thus featuring a great potential of the selected approach for the synthesis of organic semiconductor polymers.

Scheme 1 shows the synthesis of polymers **P–Sz**, **P–St** by Suzuki and Stille condensation and **P–C** by thermally induced condensation of **M5** with dithioxamide under microwave irradiation.[13] Monomers **M1–M5** were obtained by previously reported methods[17–20] (for details, see Online Supplementary Materials). Since the monomers possess very different solubility in polar and non-polar solvents, it was challenging to select the optimal system where the starting compounds and the resulting polymer would be simultaneously well-soluble. We investigated an effect of solvents with different physicochemical properties (boiling point, dielectric constant, *etc.*) on the molecular weight of the resulting polymers in the reaction between monomer

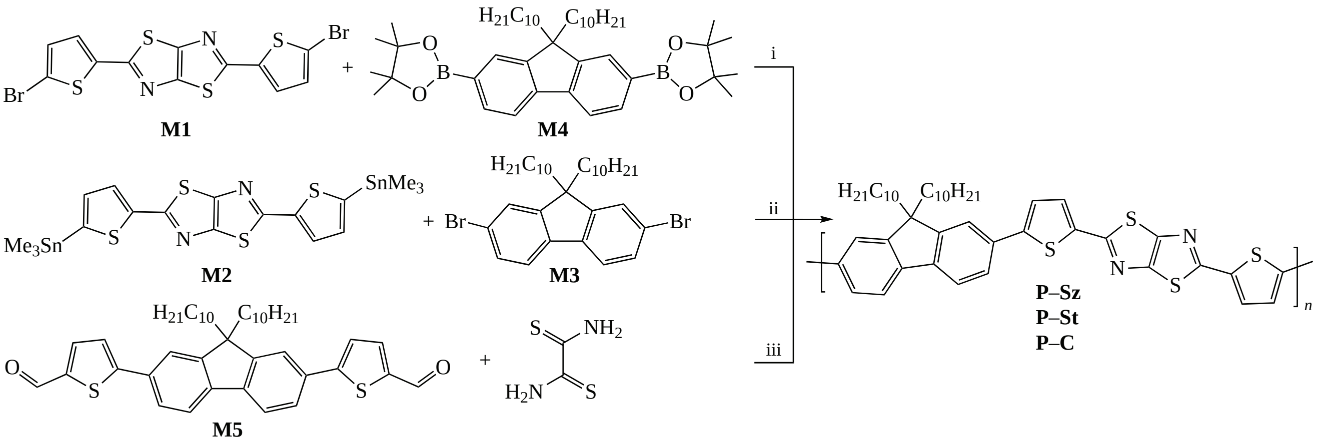

Scheme 1 *Reagents and conditions*: i, $Pd(PPh_3)_4$, 2 M K_2CO_3, Aliquat 336, toluene, reflux; ii, $Pd_2(dba)_3$, $P(C_6H_4Me\text{-}o)_3$, toluene, reflux; iii, DMF, microwave 600 W.

M5 and dithioxamide (see Online Supplementary Materials, Table S1). The polymers obtained in 1,2-dichlorobenzene, THF, and *o*-xylene had the lowest molecular weights. The average molecular weight M_w showed growth during the first hour after the start of the reaction and did not exceed 3.0 kDa. When using dioxane and *N*,*N*-dimethylacetamide, the M_w value exhibited a minor increase up to 4.0 kDa. At the same time, precipitation of products was observed. In DMF, the low-soluble viscous resin-like product (M_w of 18.6 kDa) was formed after 16 min from the reaction start. In pyridine, the reaction proceeded very slowly: in 10 h, the M_w of the product was about 5.0 kDa. Thus, we combined these solvents and performed the reaction in binary system that resulted in **P–C** polymer with M_w of 11.2 kDa (Table 1). All polymers were purified from low-molecular weight compounds and polar substances in a Soxhlet apparatus using acetone and dichloromethane as the extractants. The yield of polymers after purification was in the range of 35–45%. Molecular weights were in the range of 5–11 kDa, and polydispersity indexes were of 1.5–2.0. The resulting polymers showed good solubility (> 40 mg ml^{-1}) in chloroform, chlorobenzene, and 1,2-dichlorobenzene, that may allow one to use them for fabrication of thin-film electronic devices by solution processing techniques.

The ^{1}H NMR study of the polymers obtained showed that their backbone structure was similar for all samples; however, the residual signals of the characteristic functional groups for the corresponding reactants were detected (see Figure S13 and detailed discussion in Online Supplementary Materials). In particular, sample **P–St** contained some residual $SnMe_3$ groups (also confirmed by elemental analysis), however, this may turn advantageous to use them as traps for charge carriers.[21] Fourier-transform infrared spectroscopy (FTIR) also showed similarity of the samples due to the presence of the proper bands (see Figure S14 and detailed discussion in Online Supplementary Materials). The spectrum of sample **P–C** contained low-intense band at 1663 cm^{-1} which can be assigned to residual carbonyl groups.

Thermal gravimetry and differential scanning calorimetry (DSC) study of polymers **P–Sz**, **P–St**, **P–C** (see Table 1 and Online Supplementary Materials, Figure S1) showed that they had high thermal stability. The 5% weight loss was found in the range of 370–390 °C. It is of note that all polymers undergo two-step destruction. The DSC curves did not show any phase transitions. Only low intensity peak in the broad temperature range of 140–170 °C can be seen, which may be associated with weak self-ordering of polymer chains in solid state.

The optical properties of the polymers were investigated in chlorobenzene solution and thin films (see Table 1 and Figure 1). The absorption bands at shorter wavelengths (300–370 nm) correspond to π–π* transition in the polymers, while the bands at longer wavelengths (370–650 nm) can be attributed to the intramolecular charge transfer (ICT) that is typical for push–pull compounds. We expected that polymers possessing the same structure should also exhibit similar optical properties. However, some differences in absorption spectra can be observed.

Photoluminescence (PL) spectra were measured under excitation of samples using blue laser (405 nm). In the PL spectra of polymer solutions, three pronounced emission peaks at 530, 570, 605 nm can be detected (see Table 1). This may be due to three different transitions from the excited state to the ground state at different vibrational levels. The **P–St** and **P–C** polymers have higher intensity signals at 530 and 570 nm and lower intensity at 605 nm. The **P–Sz** polymer has a more pronounced peak at 605 nm, and less intense at 530 nm. Most probably, residual terminal trimethylstannyl group and carbonyl group

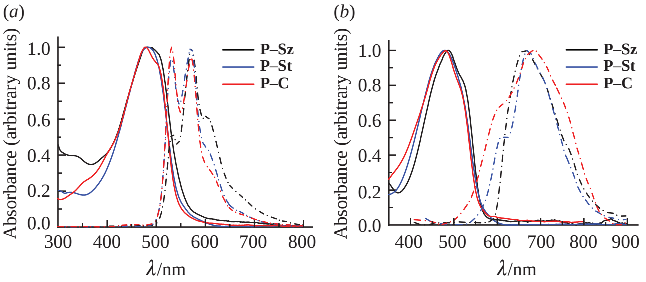

Figure 1 Absorption spectra and photoluminescence spectra of polymers **P–Sz**, **P–St**, **P–C** in (*a*) chlorobenzene solution and (*b*) thin films.

Table 1 Physicochemical, optical, and electrochemical properties of polymers **P–Sz**, **P–St**, **P–C**.

Sample	M_w/kDa	M_w/M_n	T_d/°C	Absorbance, λ^{max}/nm^a	Photoluminescence, λ^{max}/nm^a	E_g/eV	E^{ox}_{onset}/V^b	HOMO/eV	LUMO/eV
P–Sz	7.0	1.5	367	484/480	571/662	2.2	0.33	–5.13	–3.03
P–St	4.8	1.6	391	484/479	571/671	2.2	0.38	–5.18	–2.98
P–C	11.2	2.0	367	484/479	530, 571/684	2.2	0.36	–5.16	–3.96

^{a} In solution/in film, respectively. ^{b} *vs*. Fc$^+$/Fc.

enhanced the luminescence at 530 nm and quenched it at 605 nm.[22] In the PL spectra of thin films, the Stokes shifts were found to be 5728, 5930 and 6214 cm^{-1} for **P–Sz**, **P–St** and **P–C**, respectively. As in the solution spectra, the **P–Sz** polymer does not have a pronounced shoulder at 600 nm, in contrast to the **P–St** and **P–C** polymers. The relatively large Stokes shift indicates that the polymer has different ground and excited states due to the partial loss of energy (vibrational relaxations of the macromolecules). In general, the polymers have very similar emission spectra, which also indicates similarity of their electronic structure.

Next, we investigated the electrochemical properties of polymers using cyclic voltammetry (see Table 1 and Online Supplementary Materials, Figure S2). The onset oxidation potentials (E^{ox}_{onset}) were measured against Ag/Ag^+ reference electrode using ferrocenium/ferrocene (Fc^+/Fc) redox couple with the absolute energy of –4.80 eV *vs.* vacuum as an internal standard.[23] The HOMO energy levels of the polymers were determined from the oxidation onsets as $HOMO = –(E^{ox}_{onset} + 4.8)$ eV.[24] The polymers have similar HOMO energy levels in the narrow range from –5.13 to –5.16 eV. Sufficiently high HOMO energies allow one to use these polymers as hole-transport materials (HTMs) in perovskite solar cells. In sum, the similar optoelectronic and thermal properties of compounds confirm the comparable structure of the backbone of three polymers.

When developing novel materials for organic and hybrid electronic devices, their charge transport properties are of great importance. Hole mobilities (μ_h) of polymers **P–Sz**, **P–St** and **P–C** were measured by space charge limited current (SCLC) technique in hole-only devices with the following architecture ITO/PEDOT:PSS/**Polymer**/MoO_3/Ag. The μ_h values were calculated from the Mott–Gurney square law $J = (9/8)e_0 e_r m_h (V^2/L^3)$, where ε_0 was vacuum permittivity, ε_r was the dielectric constant of polymers (generally, 3.0–3.5 for organic semiconductors), μ_h was the hole mobility, V was the effective applied voltage, and L was the thickness of polymer films. The *J–V* curves are shown in Figure 2(*a*). The highest charge carrier mobility of 1.05×10^{-4} $cm^2 V^{-1} s^{-1}$ was shown by polymer obtained *via* the Suzuki reaction (Table 2). The slightly lower μ_h values of 6.33×10^{-5} $cm^2 V^{-1} s^{-1}$ were measured for the **P–St**. The polymer obtained by the alternative method demonstrates the lowest mobility $\mu_h = 5.62 \times 10^{-5}$ $cm^2 V^{-1} s^{-1}$ that may be associated with the residual carbonyl groups, which act as 'sticking centers' for charge carriers.

Finally, we investigated polymers **P–Sz**, **P–St**, **P–C** as hole-transport materials in perovskite solar cells (PSCs) in order to understand the influence of the synthetic pathway on the semiconductor properties of compounds. In particular, they were evaluated in PSCs with n-i-p architecture of ITO/SnO_2/[6,6]-phenyl-C_{61}-butyric acid (PCBA)/$MAPbI_3$/**Polymer**/MoO_3/Ag. The detailed device fabrication procedure described in Online Supplementary Materials was reported previously.[25] The thin films of polymers **P–Sz**, **P–St**, **P–C** were deposited by spin-coating from chlorobenzene solutions on the top of the perovskite layer using preliminary optimized deposition conditions. Polymer **PTAA** was used as a reference HTM. The *J–V* curves of the best devices are shown in Figure 2(*b*), and statistical distribution of device characteristics is summarized in Table 2. It can be seen that the characteristics of PSCs are in good agreement with SCLC data. The best-performance devices included **P–Sz** (PCE = 14.2%) and **P–St** (PCE = 13.8%) polymers. The PSCs with **P–C** as HTM provided lower efficiency of 9.3%. The PCE in this case is limited by low fill factors. The drastic difference in average FFs of devices based on **P–Sz**/**St** and **P–C** could arise from residual functional groups (carbonyl fragments). To characterize the hole-extracting ability provided by the materials, we recorded steady-state photoluminescence spectra of samples of glass/perovskite/HTM and glass/perovskite as a reference. The PL maps of the samples with 8 × 20 mm size and scanning step of 0.5 mm are shown in Figure 3. The PL intensity is normalized from 0 to 30 000 counts to facilitate the comparison between the samples. For **P–C** HTM substantial increase of the photoluminescence along the surface was observed. The similar effect was reported previously.[26] Such an increase in the PL intensity may be the result of the passivation of trap states on the surface of perovskite[27] and can be attributed to the Lewis base–acid interactions between C=O group and the antisite Pb, which is supported by the higher V_{OC} and J_{SC} for **P–C** based PSCs.[28] At the same time, the **P–Sz** material enabled homogeneous quenching of PL on the substrate. As for the **P–St** material, it possesses low molecular weight characteristics and thus the higher density of defects, which could lead to recombination on traps and decrease in the current density (16.7 mA cm^{-1} average J_{SC}).

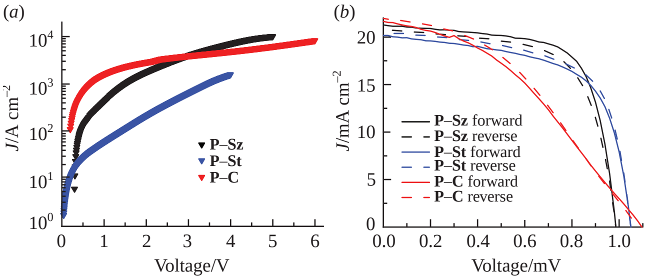

Figure 2 *J–V* curves of (*a*) hole-only devices and (*b*) PSCs.

Table 2 Photovoltaic performance of PSCs based on **P–Sz**, **P–St** and **P–C**.

Sample	V_{OC}/mV	J_{SC}/mA cm^{-2}	FF (%)	PCE (%)	μ_h/$cm^2 V^{-1} s^{-1}$
PTAA	1020[a] (995 ± 16)[b]	22.6 (21.7 ± 0.8)	74 (70 ± 2)	16.6 (15.2 ± 0.7)	3.28×10^{-5} [c]
P–Sz	1020 (995 ± 21)	20.9 (19.6 ± 1.3)	68 (63 ± 3)	14.2 (12.3 ± 1.2)	1.05×10^{-4}
P–St	1060 (1054 ± 9)	20.5 (16.9 ± 2.9)	65 (55 ± 7)	13.8 (9.9 ± 2.9)	6.33×10^{-5}
P–C	1060 (1078 ± 16)	22.6 (20.8 ± 1.8)	39 (36 ± 2)	9.3 (8.1 ± 0.6)	5.62×10^{-5}

[a] Maximal value (average ± standard deviation). [b] Average characteristics for sixteen devices. [c] From ref. 29.

We believe that the end-capping of carbonyl groups should significantly improve the semiconductor properties of **P–C** polymer. In contrast to palladium-catalyzed Stille and Suzuki reactions, metal-free condensation reaction has huge advantages since residual nanoparticles of palladium noticeably deteriorates semiconductor characteristics of conjugated polymers.[30]

In summary, we developed and synthesized a promising polymer based on alternating fluorene, thiophene, and thi-

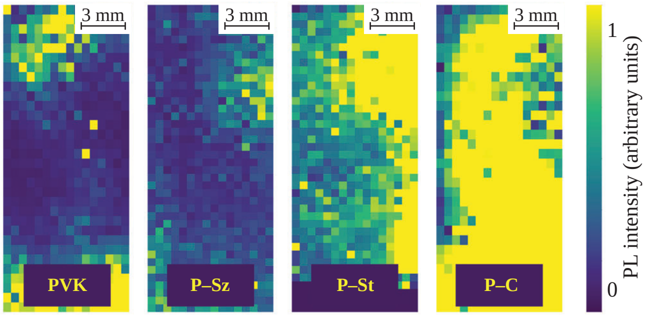

Figure 3 The photoluminescence maps of the sample glass/perovskite/HTM with 8 × 20 mm.

azolothiazole building blocks by the Stille and Suzuki cross-coupling reactions, as well as by microwave-assisted polycondensation reaction. Analysis of composition, physicochemical and optoelectronic properties of three polymers revealed their similar structure. The potential of **P–C**, **P–St** and **P–Sz** as hole-transport materials was assessed in n-i-p perovskite solar cells. Polymer **P–C** provided lower performance of perovskite solar cells due to reduced fill factors. This is attributed to inferior hole mobilities of **P–C** that in turn can be explained by the presence of residual carbonyl groups in polymer chains acting as charge traps. End-capping of polymer chains through the Knoevenagel reactions or formation of azomethine motif is regarded as possible improvement of the semiconductor properties of **P–C**. The results of our work demonstrated great potential of alternative condensation reaction in obtaining conjugated polymers without using expensive palladium-containing catalyst, toxic stannanes or poorly stable organoboron compounds featuring importance of this approach for large-scale production of organic semiconductors.

This work was funded by Russian Science Foundation (grant no. 22-73-00029). NMR measurements were performed using equipment of the Multi-User Analytical Center of the Federal Research Center of Problems of Chemical Physics and Medicinal Chemistry RAS.

Online Supplementary Materials

Supplementary data associated with this article can be found in the online version at doi: 10.1016/j.mencom.2023.09.029.

References

1 J. Yang, B. Xiao, A. Tang, J. Li, X. Wang and E. Zhou, *Adv. Mater.*, 2019, **31**, 1804699.
2 I. E. Kuznetsov, M. E. Sideltsev, V. G. Kurbatov, M. V. Klyuev and A. V. Akkuratov, *Mendeleev Commun.*, 2022, **32**, 527.
3 M. M. Tepliakova, A. N. Mikheeva, P. A. Somov, E. S. Statnik, A. M. Korsunsky and K. J. Stevenson, *Energies*, 2021, **14**, 5115.
4 A. S. Steparuk, Yu. A. Kvashnin, G. L. Rusinov, E. V. Verbitskiy, A. E. Aleksandrov, D. A. Lypenko, A. R. Tameev and V. N. Charushin, *Russ. Chem. Bull.*, 2023, **72**, 527.
5 Y. Sui, Y. Deng, T. Du, Y. Shi and Y. Geng, *Mater. Chem. Front.*, 2019, **3**, 1932.
6 J. Kim, M. Rémond, D. Kim, H. Jang and E. Kim, *Adv. Mater. Technol.*, 2020, **5**, 1900890.
7 Z. Qiu, B. A. G. Hammer and K. Müllen, *Prog. Polym. Sci.*, 2020, **100**, 101179.
8 P. M. Kuznetsov, I. E. Kuznetsov, I. V. Klimovich, P. A. Troshin and A. V. Akkuratov, *Mendeleev Commun.*, 2021, **31**, 30.
9 S. Wen, Y. Li, N. Zheng, I. O. Raji, C. Yang and X. Bao, *J. Mater. Chem. A*, 2020, **8**, 13671.
10 S. Wang, Y. Tao, S. Li, X. Xia, Z. Chen, M. Shi, L. Zuo, H. Zhu, X. Lu and H. Chen, *Macromolecules*, 2021, **54**, 7862.
11 U. Olgun and M. Gülfen, *RSC Adv.*, 2014, **4**, 25165.
12 J. A. Osaheni and S. A. Jenekhe, *J. Am. Chem. Soc.*, 1995, **117**, 7389.
13 X. Zhao, Z. He, W. Ou, P. Lin, Y. Chen and Y. Chen, *Sci. China Mater.*, 2022, **65**, 2491.
14 K. D. Belfield, S. Yao, A. R. Morales, J. M. Hales, D. J. Hagan, E. W. Van Stryland, V. M. Chapela and J. Percino, *Polym. Adv. Technol.*, 2005, **16**, 150.
15 J. R. Johnson and R. Ketcham, *J. Am. Chem. Soc.*, 1960, **82**, 2719.
16 A. Dessì, M. Calamante, A. Mordini, L. Zani, M. Taddei and G. Reginato, *RSC Adv.*, 2014, **4**, 1322.
17 I. H. Jung, J. Yu, E. Jeong, J. Kim, S. Kwon, H. Kong, K. Lee, H. Y. Woo and H.-K. Shim, *Chem. – Eur. J.*, 2010, **16**, 3743.
18 P. M. Kuznetsov, S. L. Nikitenko, I. E. Kuznetsov, P. I. Proshin, D. V. Revina, P. A. Troshin and A. V. Akkuratov, *Tetrahedron Lett.*, 2020, **61**, 152037.
19 B. A. Reinhardt, L. L. Brott, S. J. Clarson, A. G. Dillard, J. C. Bhatt, R. Kannan, L. Yuan, G. S. He and P. N. Prasad, *Chem. Mater.*, 1998, **10**, 1863.
20 B. Balan, C. Vijayakumar, S. Ogi and M. Takeuchi, *J. Mater. Chem.*, 2012, **22**, 11224.
21 J. K. Park, J. Jo, J. H. Seo, J. S. Moon, Y. D. Park, K. Lee, A. J. Heeger and G. C. Bazan, *Adv. Mater.*, 2011, **23**, 2430.
22 I. M. Abdellah and A. El-Shafei, *J. Photochem. Photobiol., A*, 2020, **387**, 112133.
23 C. M. Cardona, W. Li, A. E. Kaifer, D. Stockdale and G. C. Bazan, *Adv. Mater.*, 2011, **23**, 2367.
24 B. Lim, H. Sun, J. Lee and Y.-Y. Noh, *Sci. Rep.*, 2017, **7**, 164.
25 M. M. Tepliakova, I. E. Kuznetsov, I. A. Avilova, K. J. Stevenson and A. V. Akkuratov, *Macromol. Chem. Phys.*, 2021, **222**, 2100136.
26 A. N. Mikheeva, I. E. Kuznetsov, M. M. Tepliakova, A. Elakshar, M. V. Gapanovich, Y. G. Gladush, E. O. Perepelitsina, M. E. Sideltsev, A. F. Akhkiamova, A. A. Piryazev, A. G. Nasibulin and A. V. Akkuratov, *Molecules*, 2022, **27**, 8333.
27 Q. Jiang, Y. Zhao, X. Zhang, X. Yang, Y. Chen, Z. Chu, Q. Ye, X. Li, Z. Yin and J. You, *Nat. Photonics*, 2019, **13**, 460.
28 R. Wang, J. Xue, K.-L. Wang, Z.-K. Wang, Y. Luo, D. Fenning, G. Xu, S. Nuryyeva, T. Huang, Y. Zhao, J. L. Yang, J. Zhu, M. Wang, S. Tan, I. Yavuz, K. N. Houk and Y. Yang, *Science*, 2019, **366**, 1509.
29 Y. Ko, Y. Kim, C. Lee, Y. Kim and Y. Jun, *ACS Appl. Mater. Interfaces*, 2018, **10**, 11633.
30 P. A. Troshin, D. K. Susarova, Y. L. Moskvin, I. E. Kuznetsov, S. A. Ponomarenko, E. N. Myshkovskaya, K. A. Zakharcheva, A. A. Balakai, S. D. Babenko and V. F. Razumov, *Adv. Funct. Mater.*, 2010, **20**, 4351.

Received: 27th April 2023; Com. 23/7158